

## NUMERICAL SIMULATIONS OF HYDROFORMING OF A Y-SHAPE BRANCH

RAFAL STADNIK, JAN KAZANECKI

AGH University of Science and Technology

### Abstract

The hydroforming process offers several advantages as compared with conventional manufacturing via stamping and welding, such as part consolidation, weight reduction, improved structural strength and stiffness, lower tooling costs, fewer secondary operations, tight dimensional tolerances, low springback, and reduced scrap. In this study, the estimation of the process parameters for hydroformed Y-shapes (i.e. pressure levels, axial feed and counter punch force) is discussed. Application of the simulation methods to the development of the hydroforming parts is illustrated. Numerical simulations of the tubular Y-shape element were conducted using the commercial ABAQUS explicit finite element code.

**Key words:** Tube hydroforming, FEA, Y-shape

### 1. INTRODUCTION

Hydroforming technology is a process which was first employed to form sheets by the use of liquid as a soft punch. In recent years, with the reduction of cycle time and process controls improvement, the field of applications of hydroforming has grown considerably. The most significant application of hydroforming is in the automotive industry. The demand for weight reduction in modern vehicle construction has led to an increase in the application of hydroforming process for the manufacture of automotive lightweight component made from steel and aluminium. Hydroforming technology can achieve weight reductions of around 30% in comparison to conventionally manufactured components (Massoni, 2002; Lück et al., 2001). One of the most widespread hydroforming technologies among industrial applications is the tube hydroforming (THF). The parts currently produced using THF are illustrated in figure 1 (Dochmann and Hartl, 2004; Lang et al., 2004):

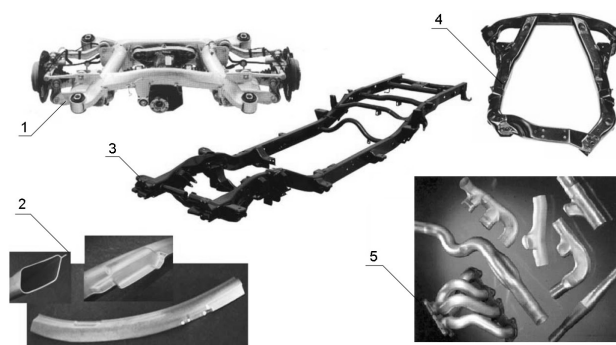


Fig. 1. Applications of hydroforming: 1) rear axle (BMW, Germany); 2) body frame part (roof rails, frame rails, etc.); 3) frame (aluminium and steel frame for car and pick-up); 4) engine subframe (Vari-Form, USA); 5) exhaust system components (Schuler Hydroforming, Germany)

In most cases, the starting work-piece is a semi-finished product. Usually this is a tube that has been roll-formed from hot or cold-rolled strip and subsequently longitudinally welded. Today, these tubes are mainly manufactured from steel and aluminium. Heat treatment and alloying additions are selected depending on application.

In this paper, the process design of hydroformed Y-shapes (3-way connectors with an angled branch) was discussed. These parts are the most common components hydroformed for exhaust system applications. The simple equations were used in order to estimate all of the necessary process parameters (e.g. internal pressure, axial feeds and initial tube length). These estimated parameters were then inserted to the FE simulations. As an initial shape for the simulations the tubular blank made from low carbon steel was used.

## 2. THE PROCESS PRINCIPLES

The initial work-piece is placed into a die cavity that corresponds to the final shape of the component. The hydroforming process occurs under the simultaneous action of an axial feed at the ends of tubular blank, and a hydrostatic internal pressure which affects the internal walls of the tubular part. These loads expand the tube wall to the die cavity (Dochmann and Hartl, 2004). In addition, hydroforming of the Y-shapes requires an application of counter punch to support the branch forming, figure 2. Because of this counter punch, the protrusion with more uniform wall thickness distribution can be formed.

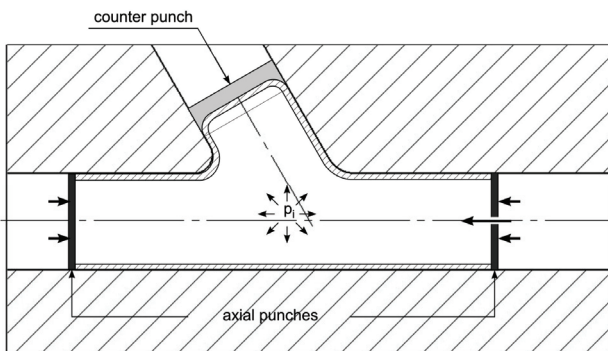


Fig. 2. Hydroforming diagram of a Y-shape

Deformation of the Y-shape in hydroforming process depends on: appropriate loading path (axial feeds, internal pressure and counter punch force vs. time); initial tube length; material and friction conditions. This is important in terms of achieving defect-free parts, robust production process conditions, and minimization of equipment capacity requirements (Koc, 2003). The goal of these simulations was to determine the best combination of counter punch force curve and pressure curve versus time such that the height of the branch was maximum. In determination of proper THF process parameters, FE simulations are usually applied in a

trial-and-error method (Jirathearanat et al., 2004a; Jirathearanat, Altan, 2004b).

## 3. GEOMETRIC PARAMETERS

During the hydroforming process, only a limited amount of material can be pushed into the die cavity. The amount of axial feeds (left stroke  $s_L$  and right stroke  $s_R$ ) necessary to form Y-shape with a desired branch height ( $H_b$ ) is approximated by equating the material volume of the hydroformed component with the material volume of tubular blank. For complex shapes, the component volume can be obtained from CAD model. The original tube wall thickness is assumed to remain unchanged (Singh, 2003). In this paper, four Y-shapes with different geometrical parameters were described. For the cases, where tube blank outside diameter ( $D_0$ ) is 50 mm, wall thickness ( $t_0$ ) has two values, 1 mm and 1,5 mm. The same situation is for  $D_0 = 20$ mm. In all cases, the Y-shapes have the same angle ( $\alpha = 60^\circ$ ), and branch diameter equal blank outside diameter ( $D_b = D_0$ ), as pictured in figure 3.

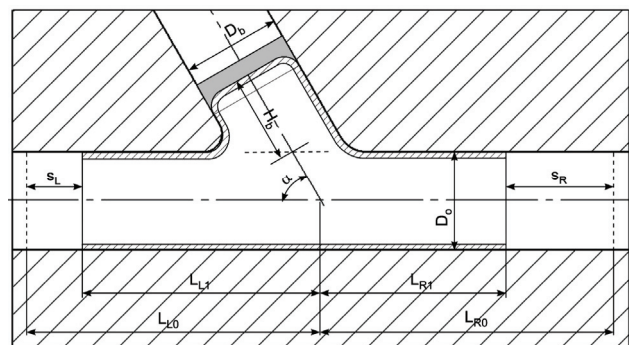


Fig. 3. Geometric parameters of the Y-shape

The relationship approximated between necessary axial strokes to the branch height ( $H_b$ ) was described by Jirathearanat et al. (2004a). They indicated that the left axial stroke ( $s_L$ ) and right stroke ( $s_R$ ) should be  $H_b$  and  $2H_b$ , respectively. Moreover, this procedure to determine the axial feeds can be applied to hydroforming of any other Y-shape geometries. When the axial feeds are estimated, the initial tube length (the sum of  $L_{L0}$  and  $L_{R0}$ ) can be calculated by adding the axial strokes ( $s_L$  and  $s_R$ ) to the final Y-shapes length (the sum of  $L_{L1}$  and  $L_{R1}$ ).

## 4. CALCULATION OF THE INTERNAL PRESSURE

In order to manufacture a part without any defect and within required dimensional tolerances, internal



pressure versus time curves need to be calculated and designed properly in coordination with axial feeding. Internal pressure ( $P_i$ ) should be (Koc, M., Altan, T., 2002a; Koc, M., Altan, T., 2002b; Koc et al., 2000; Jirathearanat et al., 2004):

- High enough to prevent wrinkling due to excessive compressive axial stroke at the initial stage of hydroforming (figure 4).
- High enough to start deformation of the tube wall at the initial stages of deformation. This yielding pressure  $(P_i)_y$ , see equation (1), is accurate for a simple tube expansion with fixed ends, but it has proved to be a good initial guess for hydroforming of more complex part with axial feed applied. It depends on the yield strength of the material ( $\sigma_y$ ), initial thickness ( $t_0$ ) and outside diameter ( $D_0$ ) of the tube.

$$(P_i)_y = \frac{2\sigma_y t_0}{D_0 - t_0} \quad (1)$$

- Low enough not to cause instability by bursting (figure 4). This bursting pressure  $(P_i)_b$ , is the maximum pressure that expands the tube without bursting, equation (2). It depends on the ultimate tensile strength of the material, initial thickness ( $t_0$ ) of the tube and branch diameter ( $D_p$ ).

$$(P_i)_b = \frac{4\sigma_u t_0}{D_p - t_0} \quad (2)$$

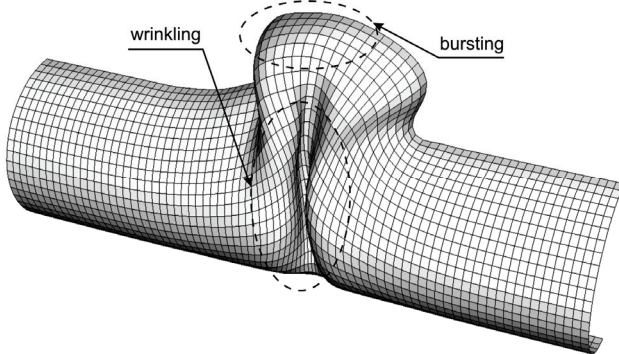


Fig. 4. Defects of the tube wall

One of the possible ways to estimate the pressure curve is its constructional determination. The calculated values of the internal pressure can be connected with a straight line, and pressure curve for the Y-shape hydroforming can be constructed. In the present study, however, the optimal pressure curve was determined through FE simulations.

## 5. COUNTER FORCE

Counter punches are used on protrusion section to avoid premature fracture by providing a controlled material flow. The use of counter force becomes particularly necessary in cases, where the amount of expansion is large, and the feeding of the material into the section by axial loads is less possible (Koc, Altan, 2002a). The counter punch enabled favorable tri-axial stress state during deformation (without counter punch there is bi-axial stress state) that avoids excessive thinning at the top of the branch and delays onset of plastic instability. Inversely, larger tube expansion can be achieved.

## 6. FE MODEL OF THE Y-SHAPES

Computer simulations of the Y-shape hydroforming process were performed using ABAQUS/Explicit software (Hibbit et al., 1998). FEA of a simple Y-shaped hydroformed part was utilized to investigate the effect of loading path on the attainable branch height and thinning limitations for four different tubular blanks. Geometrical model consists of: two dies, two axial punches, counter punch and tube (figure 5).

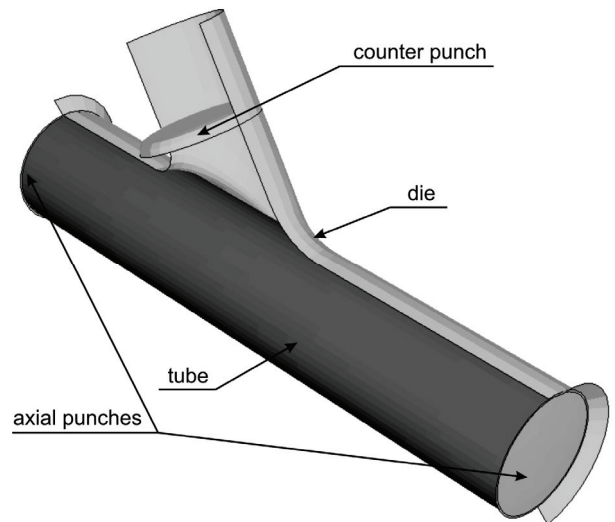


Fig. 5. Geometrical model of the Y-shape

The tube was meshed using shell elements, dies and punches were modeled as the rigid surfaces. The deformation behavior of the tube material was isotropic. The coefficient of friction is uniform at all points and equals 0,1. Table 1 presents the initial material and tube parameters used for present analysis.



Table 1. Material parameters used in the FEA of the Y-shape (DC01 steel grade)

Strength coefficient $K$ , MPa	493
Strain hardening exponent, $n$	0,1297
Young modulus $E$ , Mpa	201200
Flow stress, $\bar{\sigma} = K \bar{\epsilon}^n$	

7. RESULTS OF NUMERICAL SIMULATIONS

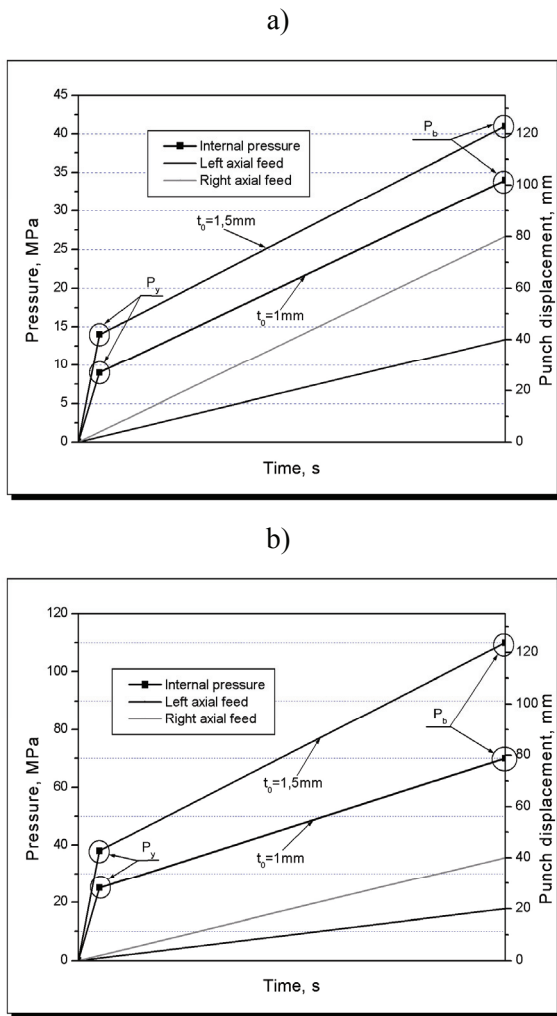


Fig. 6. Pressure and axial punches stroke vs. time for initial diameter ( $D_0$ ): a) 50 mm; b) 20 mm

The process was divided into two steps. First step was the free expansion without counter punch movements. The second step was the forming with acting force on the counter punch. The second step started when top of the branch had touched the counter punch. After the branch had come in contact with the counter punch, the counter punch went slowly upward supporting the growth of branch without excessively thinning. In whole process, axial

punches stroke was the same. Figure 6 illustrates the two different loading paths applied for two different tubular blanks, as described above.

The loading paths were obtained with the calculation of yielding and bursting pressure values using equations (1) and (2), and from geometrical parameters of the Y-shapes. For all examples pressure curves rapidly grow to yielding pressure in order to prevent wrinkling at the initial stage of hydroforming. After that, pressure slowly grows to bursting pressure. When this pressure had been reached the hydroforming process stopped.

Y-shape hydroforming for  $D_0=20\text{mm}$  and  $t_0 = 1,5 \text{ mm}$  has a failure in the form of wrinkling, as can be seen from figure 7. This failure results from high axial strokes and appears at the end of the process. Increasing the forming pressure doesn't prevent wrinkling, but causes thinning at the top of the branch. As expected, higher internal pressure restricts the material flow into the expansion zone. It is caused by increased friction force between tube and the dies. For these Y-shape dimensions any change in the loading path doesn't affect process improvement significantly. Therefore, this case was not taken into consideration in the further part of the study.

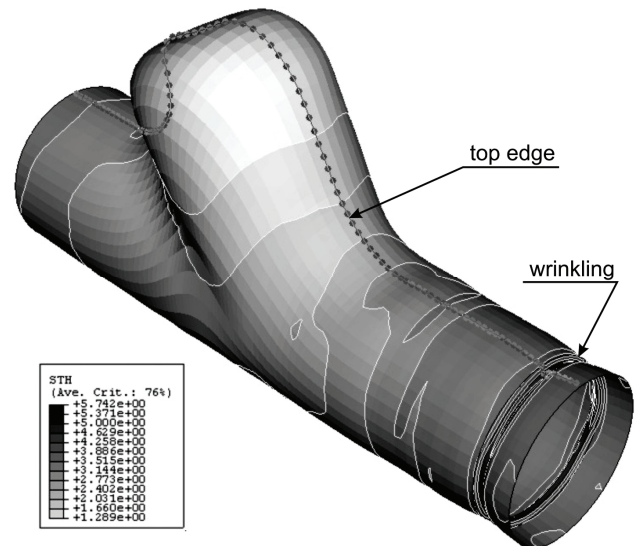


Fig. 7. Wall thickness distribution for Y-shape with a failure

Figure 8 shows a comparison of thickness variations of the Y-shape predicted with FEA for various counter punch force. As expected, maximum thickening at the end of the Y-shape was for the maximum value of the counter punch force, as well as for the  $D_0 = 20 \text{ mm}$ ,  $t_0 = 1 \text{ mm}$ . The simulation results predicted a sound Y-shape with the maximum thinning at the top of the branch, that



were 15%, 29% and 14% for ( $D_0 = 50$  mm,  $t_0 = 1,5$  mm), ( $D_0 = 50$  mm,  $t_0 = 1$  mm) and ( $D_0 = 20$  mm,  $t_0 = 1$  mm), respectively.

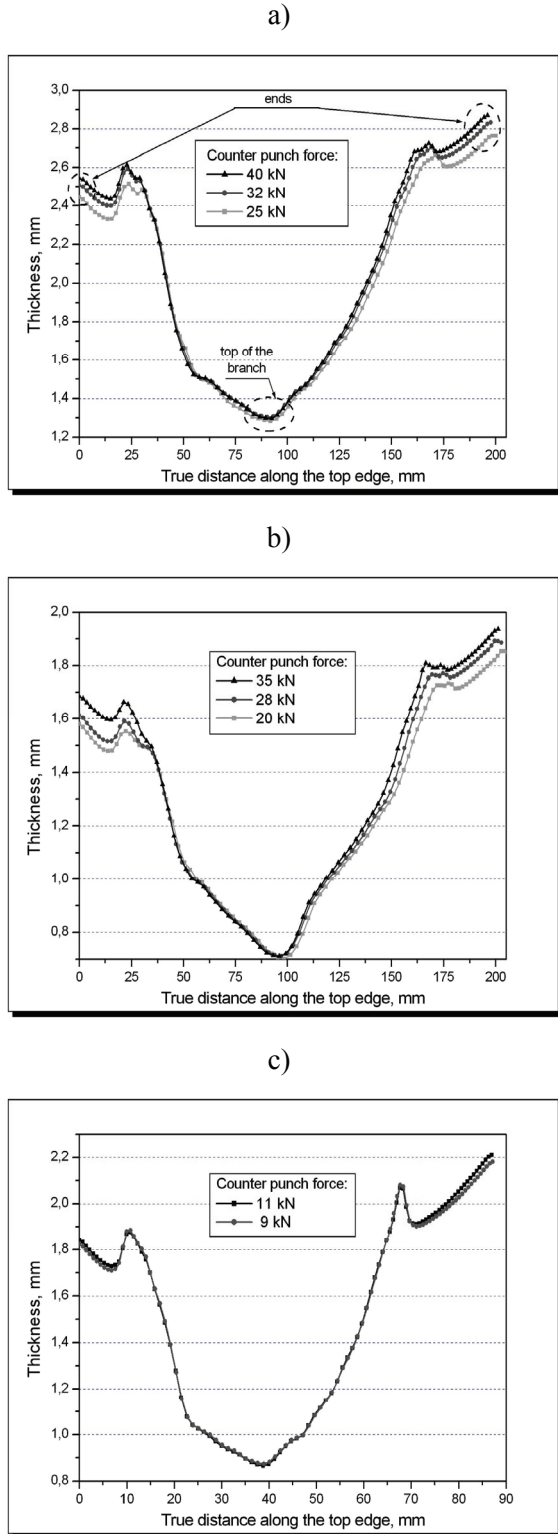


Fig. 8. Comparison of wall thickness variations along the top edge of the final part for different counter punch force: a)  $D_0=50$  mm,  $t_0=1,5$  mm; b)  $D_0=50$  mm,  $t_0=1$  mm; c)  $D_0=20$  mm,  $t_0=1$  mm

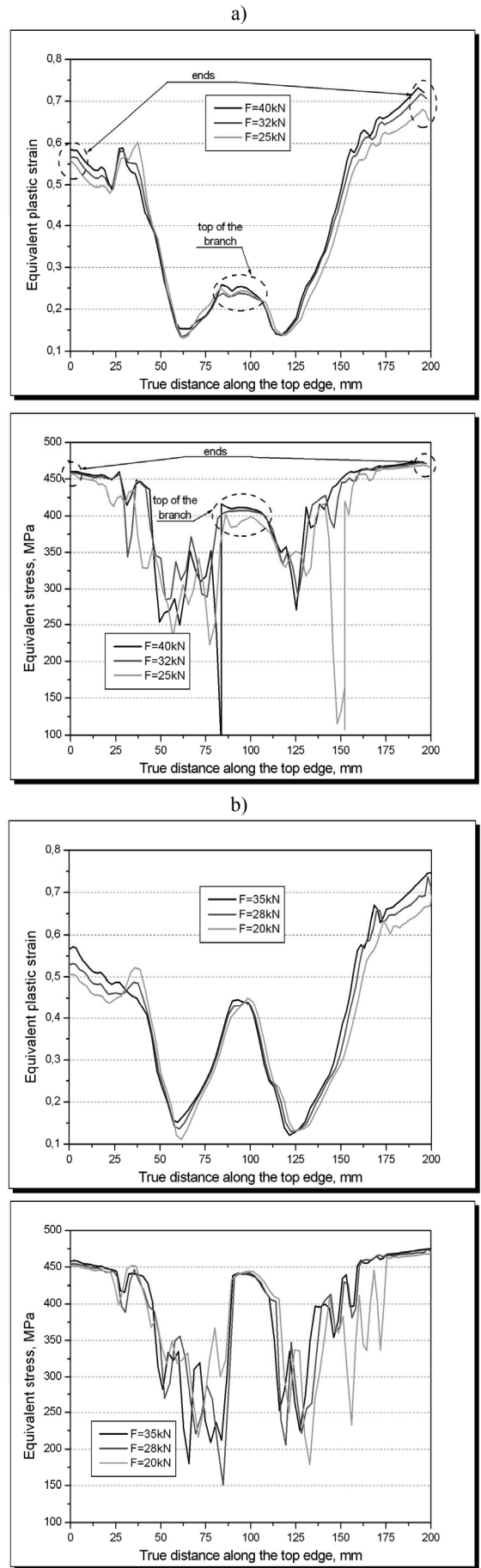


Fig. 9a-b. Equivalent plastic strain (left pictures) and stress (right pictures) variation along the top edge of the final part for: a)  $D_0=50$  mm,  $t_0=1,5$  mm; b)  $D_0=50$  mm,  $t_0=1$  mm



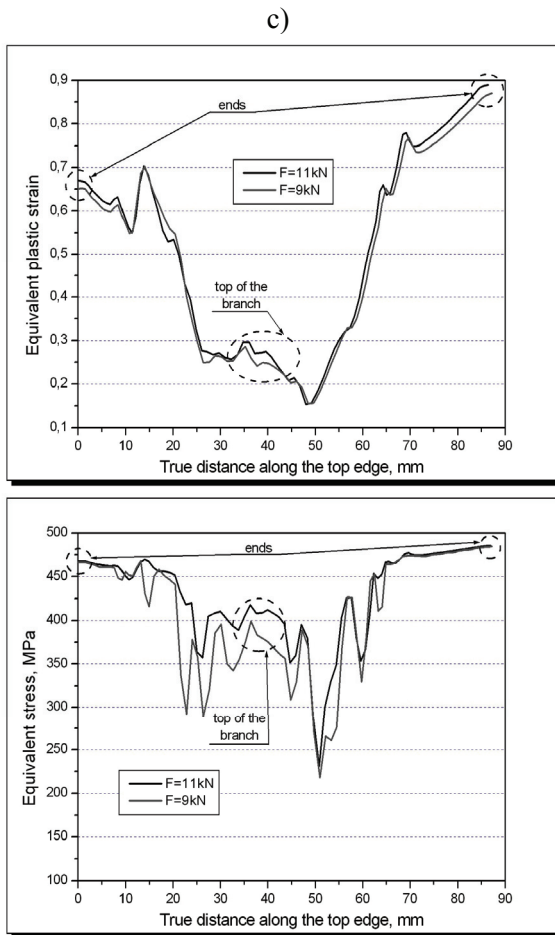


Fig. 9c. Equivalent plastic strain (left pictures) and stress (right pictures) variation along the top edge of the final part for: c)  $D_0=20$  mm,  $t_0=1$  mm

Figure 9 shows equivalent plastic strain and equivalent stress variations along the top edge of the Y-shape for all cases. For a different diameters and wall thicknesses of the tubular blank, as seen from figure 9, three points of final part can be selected (two ends of the Y-shape and the top of the branch), where the largest differences in the values of the equivalent strain and equivalent stress are observed. For tubular blank  $D_0=20$  mm and wall thickness  $t_0=1$  mm these differences have maximum values. Comparing these results with Stadnik and Kazanecki (2006), it can be stated that decreasing the diameter of the tubular blank, makes these differences more visible. In this work authors conducted numerical simulations for X5CrNi18-10 stainless steel.

Moreover, figure 10 shows the different counter forces obtained from different branch heights and geometrical parameters of the Y-shapes. It can be seen that the maximum value of the branch heights corresponds to the minimum value of the counter force.

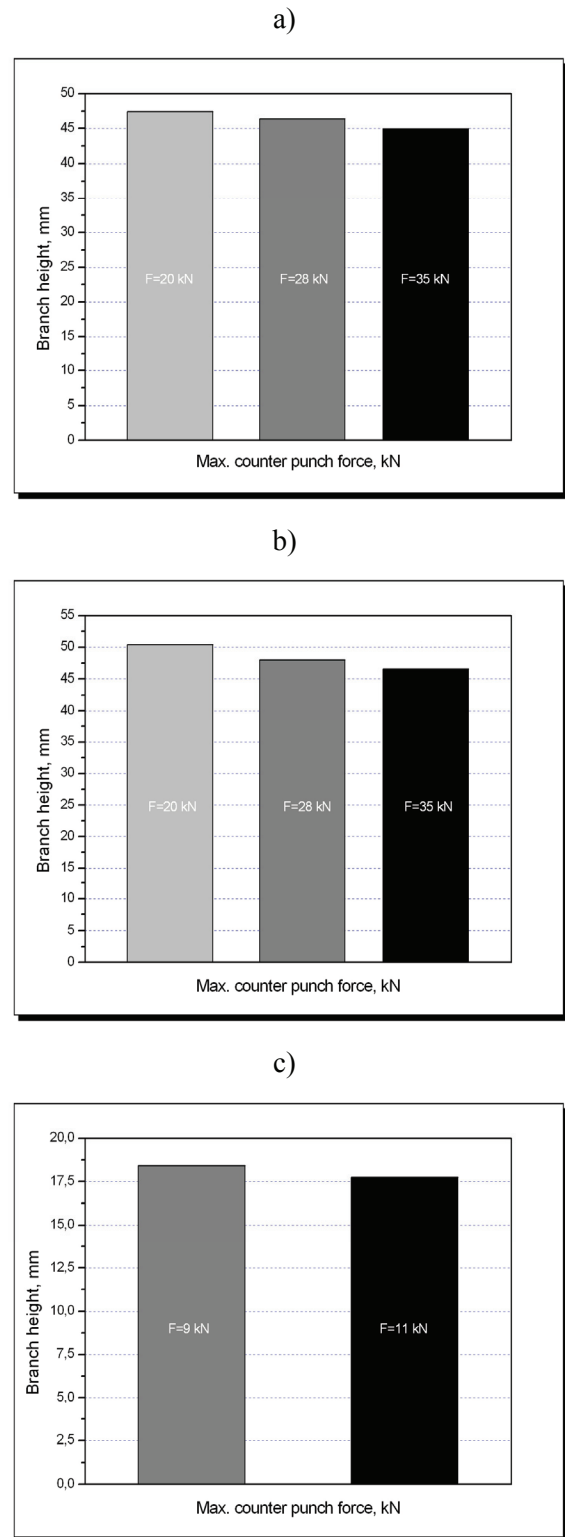


Fig. 10. Different counter forces for different branch heights: a)  $D_0=50$  mm,  $t_0=1,5$  mm; b)  $D_0=50$  mm,  $t_0=1$  mm; c)  $D_0=20$  mm,  $t_0=1$  mm

### 8. CONCLUSIONS

Coordination of the internal pressure, axial feeding and counter punch force is a crucial task in achieving the maximum height of the branch without any defects. Reduction of the branch height causes increase in the counter punch force. In all cases



thinning for the respective diameters and wall thickness of the tube at the top branch remains almost the same, even when the largest counter punch force is applied. Moreover, at the end of the Y-shapes thickening increased. The results of these simulations show that increase in the counter punch force doesn't affect the thickening at the top of the branch.

Wall thickness of the tube made from low carbon steel is a crucial factor for successful process. For tube with a small diameter and too large wall thickness hydroforming of a Y-shapes was unsuccessful. It can be concluded that the proper selection of the material and geometrical parameters, especially for the small diameter of low carbon steel Y-shape is one of the most important issues.

## ACKNOWLEDGEMENTS

The work was performed with financial assistance of AGH project No. 11.11.110.644.

## REFERENCES

- Dochmann, F., Hartl, Ch., 2004, Hydroforming-applications of coherent FE-simulations to the development of products and processes, *J. Mat. Proc. Techn.*, 150, 18-24.
- Hibbit, Karlsson, Sorensen, 1998, ABAQUS/Explicit User's Manual, Inc.
- Jirathearanat, S., Altan, T., 2004b, Optimization of Loading Path for Tube Hydroforming, *Mat. Conf. NUMIFORM 2004*, ed. S. Ghosh, J.C. Castro, J.K. Lee, 1148-1153.
- Jirathearanat, S., Hartl, Ch., Altan, T., 2004a, Hydroforming of Y-shape – product and process design using FEA simulation and experiments, *J. Mat. Proc. Techn.*, 146, 124-129.
- Koc, M., 2003, Investigation of the effect of loading path and variation in material properties on robustness of tube hydroforming process, *J. Mat. Proc. Techn.*, 133, 276-281.
- Koc, M., Allen, T., Jirathearanat, S., Altan, T., 2000, The use of FEA and design of experiments to establish design guidelines for simple hydroformed parts, *Int. J. Mach. Tools & Manufacture*, 40, 2249-2266.
- Koc, M., Altan, T., 2002a, Prediction of forming limits and parameters in the tube hydroforming process, *Int. J. Mach. Tools & Manufacture*, 42, 123-138.
- Koc, M., Altan, T., 2002b, Application of two dimensional (2D) FEA for the tube hydroforming process, *Int. J. Mach. Tools & Manufacture*, 42, 1285-1295.
- Lang, L.H., Wang, Z.R., Kang, D.C., Zhang, S.J., Danckert, J., Nielsen, K.B., 2004, Hydroforming highlights: sheet hydroforming and tube hydroforming, *J. Mat. Proc. Techn.*, 151, 165-177.
- Lück, H.-U., Hartl, Ch., Abbey, T., 2001, Hydroforming, *J. Mat. Proc. Techn.*, 115, 87-91.
- Massoni, E., 2002, Finite element simulation of hydroforming process, *Proc. Int. Conf. ESAFORM 2002*, 703-706.
- Singh, H., 2003 Fundamentals of Hydroforming, *Society of Manufacturing Engineers, USA*.
- Stadnik, R., Kazanecki, J., 2006, Hydroforming of a Y-shape branch, *Mat. Conf. KomPlasTech2006*, ed. D.Szeliga, M. Pietrzyk, J. Kusiak, s. 327 – 334.

## SYMULACJE NUMERYCZNE TRÓJNIKA Z ODGAŁĘZIENIEM KĄTOWYM

### Streszczenie

Rozpęczanie hydromechaniczne oferuje wiele zalet w porównaniu do tradycyjnych metod wytwarzania jakimi są np. tłoczenie i zgrzewanie. Zalety te wynikają m. in. z: łączenia części, zmniejszenia masy, ulepszonej wytrzymałości i sztywności konstrukcyjnej, zmniejszonych kosztów narzędzi, małej ilości operacji pośrednich, ciasnej tolerancji wymiarowej, mniejszego sprężynowania i zmniejszonej ilości odpadów. W pracy omówiono sposoby wyznaczania parametrów procesu, tj. poziomu ciśnienia wewnętrznego, przemieszczenia osiowego stempla oraz siły stempla oporowego, dla rozpęczania hydromechanicznego trójkąta z odgałęzieniem kątowym. Obrazowano zastosowanie symulacji numerycznych do projektowania procesu. Symulacje numeryczne wykonywane były przy użyciu komercyjnego oprogramowania ABAQUS.

Received: March 17, 2006

Received in a revised form: June 5, 2006.

Accepted: June 12, 2006

